Topological phases in two-legged Heisenberg ladders with alternating interactions

Greta Ghelli,[1] Giuseppe Magnifico,[1,2] Cristian Degli Esposti Boschi,[3] and Elisa Ercolessi[1,2]
[1]*Dipartimento di Fisica e Astronomia dell'Università di Bologna, I-40127 Bologna, Italy*
[2]*INFN, Sezione di Bologna, I-40127 Bologna, Italy*
[3]*CNR-IMM, Sezione di Bologna, I-40129 Bologna, Italy*

(Received 6 September 2019; revised manuscript received 6 January 2020; accepted 31 January 2020; published 14 February 2020)

We analyze the possible existence of topological phases in two-legged spin ladders, considering a staggered interaction in both chains. When the staggered interaction in one chain is shifted by one site with respect to the other chain, the model can be mapped, in the continuum limit, into a nonlinear sigma model NLσM plus a topological term which is nonvanishing when the number of legs is two. This implies the existence of a critical point which distinguishes two phases. We perform a numerical analysis of energy levels, parity, and string nonlocal order parameters, correlation functions between x, y, z components of spins at the edges of an open ladder, the degeneracy of the entanglement spectrum, and the entanglement entropy to characterize these two different phases. We identify one phase with a Mott insulator and the other one with a Haldane insulator.

DOI: 10.1103/PhysRevB.101.085124

I. INTRODUCTION

A Heisenberg spin model and its anisotropic variants (for a review, see Ref. [1] and references therein) represent an ideal playground for the description of quantum phases of matter [2] with magnetic degrees of freedom. In the special case of one-dimensional models, these systems exhibit both gapless and gapped phases, with para-, ferro-, or antiferromagnetic (AFM) correlations, and have been extensively used as a benchmark to develop new analytical or perturbative techniques. In particular, the spin $s = 1/2$ SU(2) AFM Heisenberg chain, which was known to be exactly solvable [3] and to correspond to a critical model (with a nonmagnetic ground state with short-range correlations only), has been assumed for decades as a paradigm. Thus, it came as a surprise when, in 1982, Haldane [4,5] argued that the spin $s = 1$ chain is instead gapped. Indeed, Haldane's conjecture states that there is a substantial difference between half-integer and integer spin chains. Such different behaviors can be explained in a semiclassical approach which makes use of spin coherent states [6] by mapping the model, in the continuum and low-energy limit, to an effective $O(3)$ nonlinear sigma model (NLσM) [4,5,7] plus a topological term [8,9], whose coefficient θ is proportional to the value of the spin s. For half-integer spins, the topological term is an odd multiple of π and thus weights the different topological sectors with an alternating sign, giving rise to a massless spectrum [10]. On the contrary, the topological term is a multiple of 2π and thus is ineffective for integer spin, resulting in a pure $O(3)$ NLσM, which is a massive theory characterized by a finite correlation length [11].

Actually, Haldane's argument relied on the assumption that the spin was large, but, mainly based on numerical checks, it was expected that its conclusions could also be extended to lower spins, down to $s = 1$. In 1987, Affleck, Kennedy, Lieb, and Tasaki [12] introduced the so-called AKLT model, for which the exact ground state and the existence of the Haldane gap was obtained analytically. This was just the first example of a class of models exhibiting gapped phases which were soon proved to be characterized by [13,14] hidden symmetries and nonlocal order parameters (NLOPs). Similar to what happens for the classical XY model and its Berezinskii–Kosterlitz–Thouless (BKT) transition [15,16], it was known that for all these quantum Hamiltonians, containing short-range interactions only, the Mermin-Wagner theorem [17,18] would prevent the breaking of any continuous [SU(2) or $U(1)$] symmetry, yielding instances of what we now call symmetry-protected topological (SPT) order, in which the standard framework of the Ginzburg-Landau theory [19] is not applicable. This is similar to what was then recognized to happen in a variety of models with fermions [20–24], including topological insulators and superconductors [25,26]. Recently, it has been pointed out [27,28] that a suitable class of NLOPs might provide a complete classification for fermionic models as well [29], at least in the weak coupling regime, as long as they might be dealt within a bozonization approach and mapped to a sine-Gordon theory [30].

The Heisenberg model in the two-dimensional case is very different [31–35]: The topological term is absent whatever the spin is and whatever the topology of the bipartite lattice is. To have a behavior similar to what happens in one dimension, one should examine quasibidimensional models such as coupled chains, i.e., spin ladders. For Heisenberg ladders, a generalized "even-odd conjecture" was put forward [36], according to which ladders with integer spin are gapped, while ladders with half-integer spin are gapless if the number of legs is odd and gapped if the number of legs is even, a fact strongly supported by numerical checks [37–43]. The existence of topological features as the cause of this different behavior in spin ladders was investigated in Refs. [44,45]. AFM spin ladders were studied in Ref. [46] by using bosonization techniques, while, following the original Haldane's mapping, Dell'Aringa *et al.* in Ref. [47] and Sierra in Refs. [48,49] mapped the Heisenberg Hamiltonian of a spin ladder into a NLσM which contains a topological term whose coefficient θ is proportional to both spin and number of legs, proving the above-mentioned conjecture.

It is also known that a way to control the coefficient in front of the topological term in an independent way with respect to the value of the spin is by introducing alternating interactions. This has been considered, for example, [49–51] for the one-dimensional chain and in Ref. [52] for ladders, showing that in all cases a critical point is expected for the value of the parameter controlling the alternated interactions, which yields a coefficient of the topological term $\theta_c = \pi$. Such a critical point separates two different gapped phases whose properties we want to investigate in this paper. In particular, we will show that it is indeed the presence of the topological term in the NLσM of the corresponding effective continuum field theories that controls the emergence of a phase with an SPT order, which shows up for $\theta > \theta_c$. We remark that a similar connection between topological terms in the continuum effective Lagrangian and the appearance of a SPT phase has also been found in a one-dimensional fermionic system which aims at describing a generalization of the lattice version of a Schwinger model for 1 + 1-dimensional quantum electrodynamics [53,54].

The paper is organized as follows. In Sec. II, we present our Hamiltonian of a two-legged spin ladder, with alternated Heisenberg interactions along each chain. Following Refs. [47,50], we sketch the derivation of its continuum limit low-energy effective theory, finding a NLσM plus a topological term which is nonvanishing even if the number of legs is two. This allows us to verify the results of Refs. [52,55], which predict a critical point for a certain value of the parameter which controls the alternation.

In Sec. III, we start the numerical analysis, which confirms the existence of such a critical point, separating two different gapped phases. One of these phases (for $\theta > \theta_c = \pi$) is characterized by a set of zero modes degenerate with the ground state. On the contrary to what happens in other Heisenberg ladder models characterized by some nontopological zero energy modes [56], in our case we prove that the phase with zero modes encodes an SPT order investigating NLOP, namely, parity and string NLOPs. Furthermore, in the phase with zero modes, we also check that spin correlation functions between spins at the ends of the ladder are different from zero, supporting the idea that we are in the presence of edge states. Finally, we perform an analysis of the entanglement entropy and of the degeneracy of the entanglement spectrum, showing that the latter has indeed an even degeneracy in the supposed SPT phase. These results, concerning the critical point and the topological nature of one of the two phases, are also consistent with Ref. [57], where our model is studied through a Berry phase investigation.

We finally summarize our conclusions in Sec. IV. Following the classification suggested in Refs. [27–29], we can say that our numerical analysis allows us to identify the region for $\theta < \theta_c$ with a Mott insulatorlike phase, with no edge states, nonvanishing value of the parity NLOP, and an odd degeneracy of the entanglement spectrum, while the region with $\theta > \theta_c$ with a Haldane insulatorlike phase, characterized by edge states, a nonvanishing value of the string NLOP, and an even degeneracy of the entanglement spectrum.

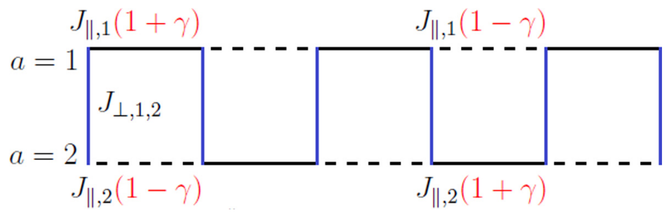

FIG. 1. Representation of model B corresponding to Hamiltonian Eq. (2), for a chain of six sites. In this figure, the coupling constants $J_{\parallel,a}$ $(a = 1, 2)$ and $J_{\perp,1,2}$ are indicated: strong and weak interchain bonds are represented by black continuous and dashed lines, while bonds between chains are in blue.

II. THE MODEL AND ANALYTICAL PREDICTIONS

We focus on two-legged spin ladders with staggered interactions along each chain. We have the choice to put the alternation in two possible different ways:

(a) In the same way on both chains, thus forming a columnar pattern of strong and weak bonds. The Hamiltonian reads

$$H = \sum_{a=1,2}\sum_{k=1}^{N} J_{\parallel,a}(1+(-1)^k\gamma)\vec{S}_{k,a}\cdot\vec{S}_{k+1,a} + \sum_{k=1}^{N} J_{\perp,1,2}\vec{S}_{k,1}\cdot\vec{S}_{k,2}, \quad (1)$$

where $S^{\alpha}_{k,a}$ $(\alpha = x, y, z)$ are the components of the spin-1/2 operator; the index $a = 1, 2$ labels the chains, while the index $k = 1, \ldots, N$ the sites along each chain. We will show that the topological term is zero in this case. This model was analytically analyzed in Ref. [58].

(b) In the opposite way, in one chain with respect to that of the second chain, yielding a staggered pattern of strong and weak bonds, as shown in Fig. 1. In this case, the Hamiltonian is

$$H = \sum_{k=1}^{N} J_{\parallel,1}(1+(-1)^{k-1}\gamma)\vec{S}_{k,1}\cdot\vec{S}_{k+1,1} + \sum_{k=1}^{N} J_{\parallel,2}(1+(-1)^{k}\gamma)\vec{S}_{k,2}\cdot\vec{S}_{k+1,2} + \sum_{k=1}^{N} J_{\perp,1,2}\vec{S}_{k,1}\cdot\vec{S}_{k,2}. \quad (2)$$

An equivalent situation is obtained by exchanging the role of the two chains. This is the case we will concentrate on, since a nonvanishing topological term will be present.

We assume that the coupling constants $J_{\parallel,1}$, $J_{\parallel,2}$, $J_{\perp,1,2}$ are all positive, so the classical minimum of the Hamiltonian is antiferromagnetically ordered, and we will work in the range $-1 \leqslant \gamma \leqslant 1$.

The partition function of both models Eqs. (1) and (2) can be expressed using a path integral representation,

$$Z = \int \mathcal{D}\hat{\Omega} \exp\left(is \sum_{k,a} \omega[\hat{\Omega}_{k,a}(\tau)] - \int_0^\beta d\tau H(\tau) \right), \quad (3)$$

with spin coherent states [6], obtained by replacing the spin operators $\vec{S}_{k,a}$ with the classical variables $s\hat{\Omega}_{k,a}(\tau)$. In Eq. (3), the first term is the Berry phase contribution, which arises as a consequence of the nonvanishing overlap between coherent states at consecutive times [59] and represents the area bounded by the trajectory parameterized by $\hat{\Omega}(\tau)$ on the S^2 sphere [7,60]. To calculate the action that appears in the phase of the exponential, we will assume Haldane's mapping [31] and follow Ref. [47] to specialize it to the case of spin ladders by taking

$$\hat{\Omega}_{k,a}(\tau) = (-1)^{a+k}\hat{\phi}(k,\tau)\left(1 - \frac{|\mathbf{l}_a(k,\tau)|^2}{s^2}\right)^{\frac{1}{2}} + \frac{\mathbf{l}_a(k,\tau)}{s}, \quad (4)$$

where the spin coherent field has been written in terms of a slow-varying field $\hat{\phi}(k,\tau)$ of unit norm, which is weighted by a staggered factor $(-1)^{k+a}$ and of uniform fluctuations $\mathbf{l}_a(k,\tau)$ which are assumed to be small, $|\mathbf{l}_a(k,\tau)|/s \ll 1$. This allows us to expand all expressions up to quadratic order in the latter field which can then be integrated out. Notice that we take $\hat{\phi}(k,\tau)$ not changing along a rung, meaning that the staggered spin-spin correlation length ξ is greater with respect to the total width of the ladder $n_l a$, a fact which is confirmed numerically [61,62]. Here we do not give further details of the calculations that can be found in Ref. [63]. For both cases A, B above, we find a partition function

$$Z = \int \mathcal{D}\hat{\phi} \exp\left(- \int dx d\tau \mathcal{L}(x,\tau) \right), \quad (5)$$

where the Lagrangian density $\mathcal{L}(x,\tau)$ is written as that of a NLσM with a topological term:

$$\mathcal{L}(x,\tau) = \frac{1}{2g}\left(\frac{1}{v_s}\dot{\hat{\phi}}^2(x,\tau) + v_s \hat{\phi}'^2(x,\tau) \right) + \frac{i\theta}{4\pi}\hat{\phi}'(x,\tau)\cdot(\hat{\phi}(x,\tau)\times\dot{\hat{\phi}}(x,\tau)). \quad (6)$$

where

$$\frac{1}{g} = \sqrt{\sum_{d,b} L^{-1}_{d,b}\left(-4s^2\gamma^2 \sum_{d,b} \alpha_{A,B} J_{\parallel,d} L^{-1}_{d,b} J_{\parallel,b} + s^2 \sum_a J_{\parallel,a} \right)},$$

$$v_s = \sqrt{\frac{\left(-4s^2\gamma^2 \sum_{d,b} \alpha_{A,B} J_{\parallel,d} L^{-1}_{d,b} J_{\parallel,b} + s^2 \sum_a J_{\parallel,a} \right)}{\sum_{d,b} L^{-1}_{d,b}}},$$

with $\alpha_A = (-1)^{(d+b)}$ and $\alpha_B = 1$ while

$$\theta_{A,B} = -4\pi s\gamma \times \left(\frac{\mp 2J_{\parallel,1}(4J_{\parallel,2} + J_{\perp,1,2}) + 2J_{\parallel,2}(4J_{\parallel,1} + J_{\perp,1,2})}{16J_{\parallel,1}J_{\parallel,2} + 4J_{\parallel,1}J_{\perp,1,2} + 4J_{\parallel,2}J_{\perp,1,2}} + \frac{\pm 2J_{\parallel,1}J_{\perp,1,2} - 2J_{\parallel,2}J_{\perp,1,2}}{16J_{\parallel,1}J_{\parallel,2} + 4J_{\parallel,1}J_{\perp,1,2} + 4J_{\parallel,2}J_{\perp,1,2}} \right). \quad (7)$$

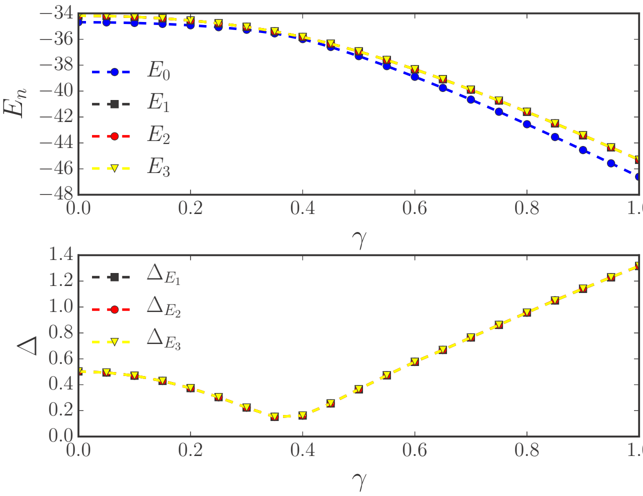

FIG. 2. The ground-state energy and the first three excited states as a function of the parameter γ (top panel) and their gaps with respect to the ground state (bottom panel) in the case of PBC. Here γ varies from 0 to 1 with a 0.05 step and we consider $N = 30$ sites for each chain.

We notice that our results are consistent with those of Ref. [47] in absence of a staggered interaction, i.e., $\gamma = 0$, which in turn are consistent with those found in Refs. [45,48,49].

As anticipated before, the topological term Eq. (7) is null for case A, yielding instead a nontrivial contribution in case B, which we will concentrate on in the following.

It is well known [64] that the NLσM is gapped for all values of the coefficient of the topological term, but for $\theta = \pi$, at which one finds a quantum phase transition [2]. In the next sections, we will check numerically that this is indeed the case and we will characterize the two phases. For simplicity, we set $J_{\parallel,1} = J_{\parallel,2} = J_{\perp,1,2} = 1$, which implies that $\theta_c = \pi$ when $\gamma_c = -0.75$. This result is the same found in Refs. [52,55].

III. NUMERICAL ANALYSIS

Our numerical analysis is based on the density matrix renormalization group algorithm [65,66] using the matrix product state tensor network (TN) [67–69].

A. Energy levels and critical point

Our first purpose is to look for the existence of a critical point, by looking at the gap. Figure 2 shows the results for periodic boundary conditions (PBCs): in the top panel, the energies of the ground state (which is in the subspace $S^z_{\text{tot}} = \sum_{a=1,2}\sum_{k=1}^N S^z_{k,a} = 0$), and of the first three excited states (which, because of the SU(2) symmetry, are degenerate and belong to subspaces $S^z_{\text{tot}} = 0$, $S^z_{\text{tot}} = +1$, $S^z_{\text{tot}} = -1$); in the bottom panel, the values of the triplet gap. The energy of the ground state is indicated with E_0, while the energies of the triplet are indicated with E_1, E_2, and E_3. Furthermore, Δ_{E_1}, Δ_{E_2}, and Δ_{E_3} are their gaps with respect to the ground state. The data have been obtained by considering $N = 30$ sites on each chain for PBC and the parameter γ varies from 0 to 1

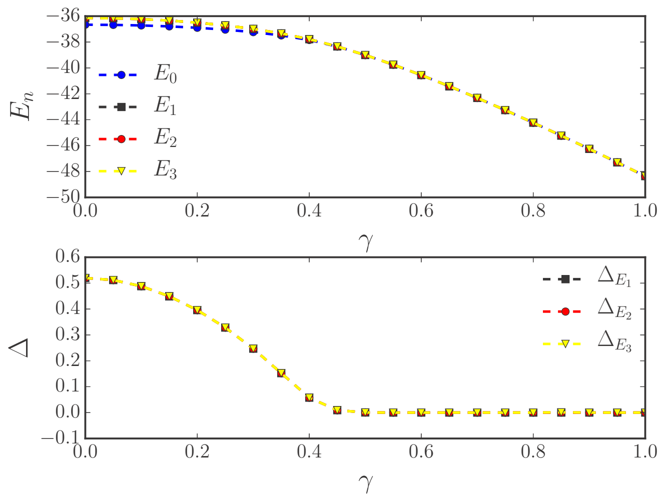

FIG. 3. The ground-state energy and the first three excited states as a function of the parameter γ (top panel) and their gaps with respect to the ground state (bottom panel) in the case of OBC. Here γ varies from 0 to 1 with a 0.05 step and we consider $N = 32$ sites for each chain.

with a 0.05 step (the model is symmetric under the inversion $\gamma \to -\gamma$).

Then, we consider open boundary conditions (OBCs). The values of the energies of the first four states and of the triplet gap are shown in Fig. 3, respectively, in the top and in the bottom panel, using the same notation of Fig. 2. We consider $N = 32$ sites on each chain and γ varying from 0 to 1 with a 0.05 step.

The data clearly show a closure of the gap for $\gamma \sim 0.35 - 0.4$. Even if the exact determination of the critical point is not our aim, we provide in the Appendix a finite-size scaling analysis for these values of γ, which confirms the existence of a critical point. It is evident that γ_c deviates a lot from the expected theoretical value $\gamma_c = 0.75$. This does not come as a complete surprise, since renormalization corrections to the semiclassical analysis performed in the previous section are expected, as also remarked in Refs. [52,55].

We also notice that the triplet states are gapped in the phase for $\gamma < \gamma_c$ while they are degenerate with the ground state in the phase for $\gamma > \gamma_c$, yielding zero modes. This is signaling that the latter phase might indeed be a SPT phase, a fact that we are now going to prove.

B. Nonlocal order parameters

Let us remark that our system is essentially a one-dimensional model with two species of spin, one for each chain. Using a Jordan-Wigner transformation [59,70], it can be interpreted as an interacting system of two fermionic species whose densities n_a/N $(a = 1, 2)$ are separately conserved. As for the Hubbard model, we have that the total z spin and total charge densities, respectively, defined as $(n_1 + n_2)/N$ and $(n_1 - n_2)/N$, are conserved. Thus, to characterize the two phases of the Hamiltonian Eq. (2) which are separated by the critical point γ_c, we can follow the work [27–29] and

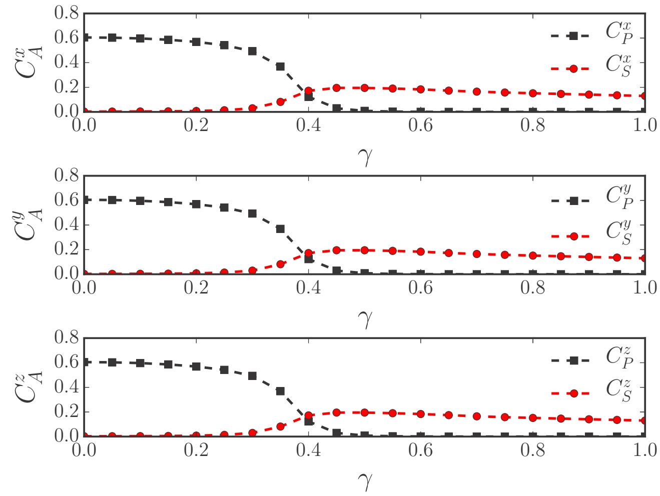

FIG. 4. Parity and string order parameters $C^{\alpha}_{P,S}$, $\alpha = x, y, z$, are shown, respectively, in black and in red, as function of the parameter γ. Here we use PBC, $N = 30$ sites on each chain and γ varies from 0 to 1 with a 0.05 step.

introduce the following two types of NLOPs, defined in terms of the parity and the string operators:

$$C^{\alpha}_P(r) = \left\langle \prod_{k=j}^{j+r-1} e^{i\pi(S^{\alpha}_{k,1}+S^{\alpha}_{k,2})} \right\rangle, \tag{8}$$

$$C^{\alpha}_S(r) = \left\langle 2S^{\alpha}_{j,1} \prod_{k=j}^{j+r-1} e^{i\pi(S^{\alpha}_{k,1}+S^{\alpha}_{k,2})} 2S^{\alpha}_{j+r,1} \right\rangle. \tag{9}$$

Notice that in all exponentials we take the sum of the spins on both chains and put a factor π, as suggested in Refs. [71,72]. The factor 2 in $C^{\alpha}_S(r)$ is introduced because it gives the correct normalization.

To reduce finite-size effects as much as possible, we consider $1 \leqslant r \leqslant \frac{N}{2}$ for PBCs and $\frac{N}{4} \leqslant r \leqslant \frac{3N}{4}$ for OBCs. For both C^{α}_P and C^{α}_S, the initial site j in and the final site $j + r$ belong to chain 1.

The behavior of C^{α}_P (black line) and C^{α}_S (red line) are given in Fig. 4 for PBCs and in Fig. 5 for OBCs, with a chain of $N = 30$ sites for PBCs and $N = 32$ for OBCs (γ always varies from 0 to 1 with a 0.05 step).

We clearly see that the SU(2) symmetry is respected, so the x, y, z components of all parameters look the same. Both with PBCs and OBCs, the parity and the string operator have a dual behavior in the two phases, with C^{α}_P nonvanishing for $\gamma < \gamma_c$ and C^{α}_S different from zero for $\gamma > \gamma_c$.

C. Correlation functions and edge states

In this subsection, we investigate spin correlation functions between the first spin of the ladder kept fixed (i.e., the first spin of the second chain) and each of the other spins of the ladder until the last one (i.e., the last spin of the second chain), when considering OBCs. To simplify the notation, we adopt a new label to number the spins along the ladder: S^{α}_J, with $J = 1, \ldots, 2N$, following a snake path, as shown in the top panel

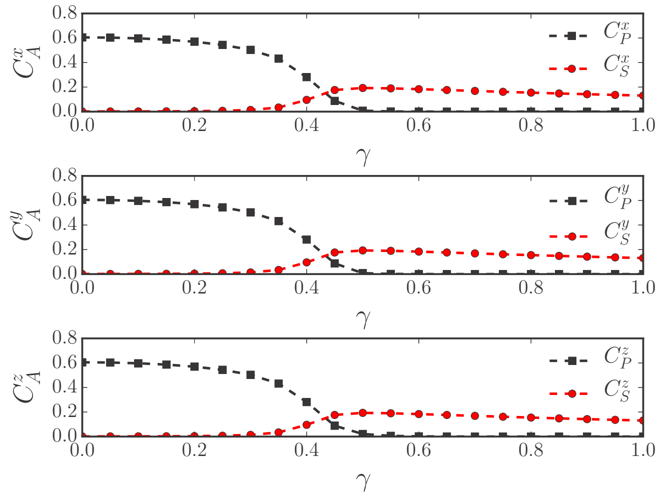

FIG. 5. Parity and string order parameters $C^{\alpha}_{P,S}$, $\alpha = x, y, z$, are shown, respectively, in black and in red, as function of the parameter γ. Here we use OBC, $N = 32$ sites on each chain and γ varies from 0 to 1 with a 0.05 step.

of Fig. 6. By using this new label, spin correlation functions can be expressed as follows:

$$CC^{\alpha}_{1,J} = \langle S^{\alpha}_1 S^{\alpha}_J \rangle, \tag{10}$$

$$CC_{1,J} = \sum_{\alpha} CC^{\alpha}_{1,J} = \langle \vec{S}_1 \cdot \vec{S}_J \rangle, \tag{11}$$

where $\alpha = x, y, z$ and $J = 1, \dots, 2N$.

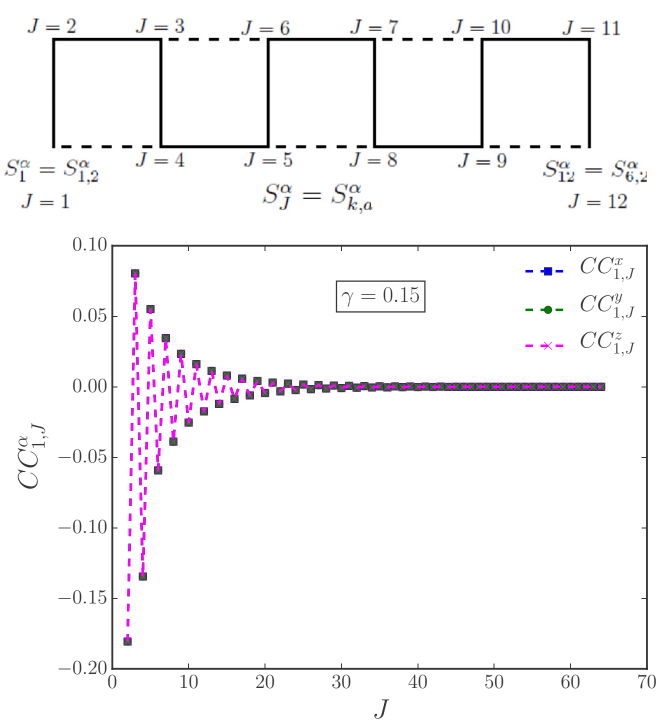

FIG. 6. Top panel: A ladder with $N = 6$ showing the new way of labeling sites using the index J, by following a snake path. Bottom panel: Ground-state spin correlations $CC^{\alpha}_{1,J}$ ($\alpha = x, y, z$), obtained with OBC, $\gamma = 0.15$ and $N = 32$ sites on each chain, i.e., 64 sites for the ladder. Correlations are calculated between the first spin ($J = 1$) of the ladder kept fixed and each of the other spins of the ladder, until the last one ($J = 2N = 64$).

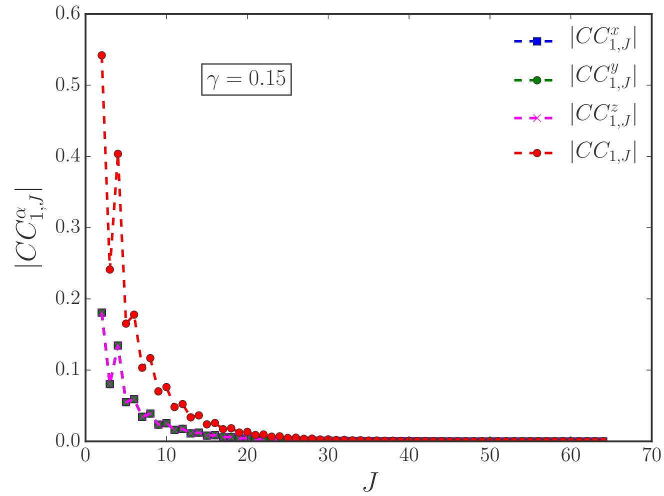

FIG. 7. Absolute value of ground-state spin correlations $|CC^{\alpha}_{1,J}|$ ($\alpha = x, y, z$) and $|CC_{1,J}|$, for OBC and $N = 32$ sites on each chain, i.e., 64 sites for the ladder. Correlations are calculated between the first spin ($J = 1$) of the ladder kept fixed and each of the other spins of the ladder, until the last one ($J = 64$), in the trivial phase for $\gamma = 0.15$.

Indeed, being in a gapped phase, we expect them to decay in an exponential way for the trivial $\gamma < \gamma_c$ case, while in the supposed topological case $\gamma > \gamma_c$ they should still decay in the bulk but have a nonzero value between the first and the last spins of the ladder, signaling the appearance of edge states.

We first notice that the SU(2) symmetry, which implies that correlation functions are identical along all three directions, is respected. Also, as expected, there is a short-range AFM order, which is evident from the staggered behavior of the correlation functions, as shown, for example, in Fig. 6. Their absolute value is plotted in Fig. 7 for the trivial case ($\gamma = 0.15$) and in Fig. 8 for the topological phase ($\gamma = 1$). In the latter case, to sort out the ground state living in the spin zero sector, we perform the numerical simulations by adding an interaction with a small magnetic field, $\mu(\sum_{J=1}^{64} \vec{S}_J)^2$, with $\mu = 10^{-3}$, to the Hamiltonian Eq. (2).

From Fig. 8, we clearly see that, for $\gamma > \gamma_c$, there is a strong correlation between the first and the last spin of the ladder, which we interpret as the emergence of zero modes made up of two entangled spins at the edges. Following the work [73] which characterizes long-distance entanglement in spin systems, we can quantify the degree of entanglement carried by such edge states by means of the concurrence between the first spin of the ladder ($J = 1$) and each of the other spins of the ladder until the last one ($J = 64$). Having an SU(2) symmetry, the concurrence can be computed as

$$C_{1,J} = \tfrac{1}{2} \max\left(0, -1 - 12\, CC^z_{1,J}\right). \tag{12}$$

We find that

$$\sum_J (C_{1,J})^2 = 0.49707302, \tag{13}$$

where the major contribution (of about 99.8%) is given by the case where J corresponds to the last spin of the ladder. We also note that this sum is smaller then 1, indicating

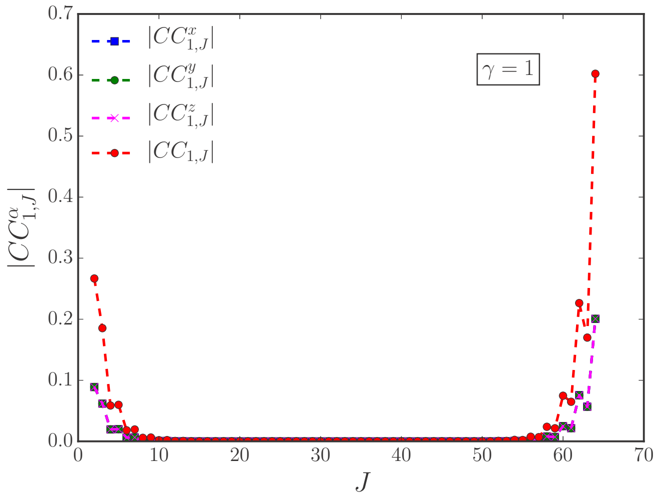

FIG. 8. Absolute value of ground-state spin correlations $|CC^{\alpha}_{1,J}|$ ($\alpha = x, y, z$) and $|CC_{1,J}|$, for OBC and $N = 32$ sites on each chain, i.e., 64 sites for the ladder. Correlations are calculated between the first spin ($J = 1$) of the ladder kept fixed and each of the other spins of the ladder, until the last one ($J = 64$), in the topological phase for $\gamma = 1$.

that the system also carries a certain degree of multipartite entanglement [74] (indeed due to rotational symmetry, all the single-site magnetizations vanish and the reduced density matrix describes a maximally entangled state of one spin with all the others).

D. Entanglement entropy and entanglement spectrum

Finally, we analyze the behavior of the entanglement entropy and the entanglement spectrum. Again using OBCs, we calculate the von Neumann entropy S_v and the spectrum of the reduced density matrix [75] obtained by tracing out half of the chain.

Figure 9 shows the values of S_v for γ from 0 to 1 with a 0.05 step, obtained for a ladder with $N = 32$ sites on each chain and OBC. We observe a clear high peak near the γ-range in which the gap in Fig. 3 closes. This is in agreement with the fact that, in the thermodynamic limit, entanglement entropy S_v diverges at the critical point γ_c.

Also, we know that at least an even degeneracy of the entanglement spectrum [75] is expected in the topological phase. In Figs. 10 and 11, we show the logarithm of the eigenvalues of the reduced density matrix greater than 10^{-12}, for $\gamma = 0.2$ and $\gamma = 0.8$, respectively, again obtained for a ladder of $N = 32$ sites on each chain. We can summarize our results by noting that the degeneracy of the entanglement spectrum changes from odd for $\gamma = 0.2$ (Fig. 10) to even for $\gamma = 0.8$ (Fig. 11), in agreement with the fact that we find a nontrivial phase for $\gamma > \gamma_c$.

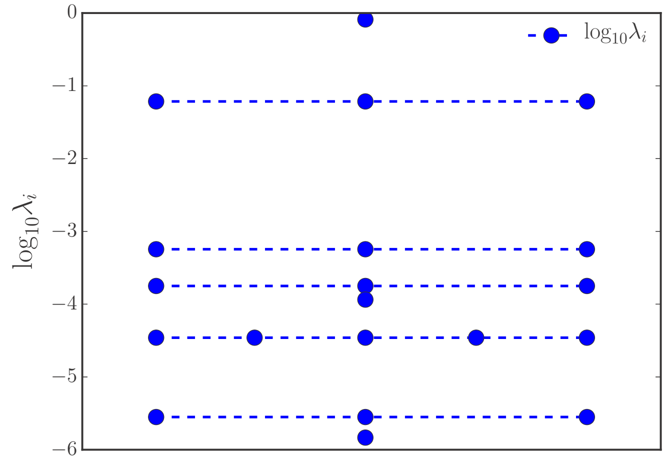

FIG. 10. Representation of the logarithm of the eigenvalues λ_i of the reduced density matrix of the system at $\gamma = 0.2$. We use OBC and $N = 32$ sites on each chain. For each value of λ_i, it is possible to see horizontally the corresponding degeneration given by the number of blue dots.

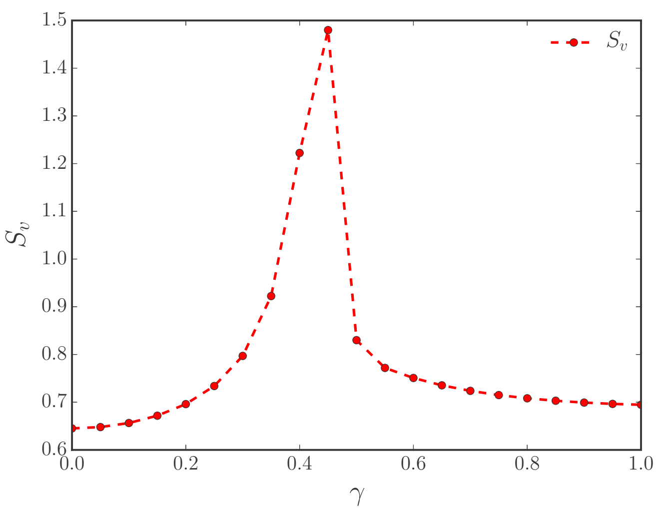

FIG. 9. Representation of entanglement entropy S_v as function of γ which goes from 0 to 1 with a 0.05 step. We use OBC and $N = 32$ sites on each chain.

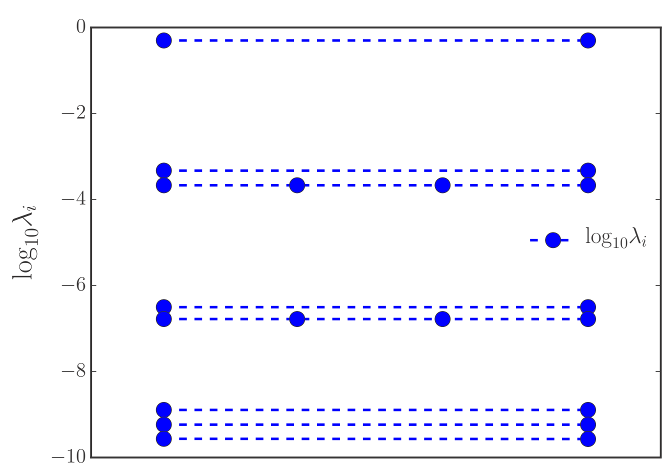

FIG. 11. Representation of the logarithm of the eigenvalues λ_i of the reduced density matrix of the system at $\gamma = 0.8$. We use OBC and $N = 32$ sites on each chain. For each value of λ_i, it is possible to see horizontally the corresponding degeneration given by the number of blue dots.

IV. CONCLUSION

We analyzed a two-legged spin ladder with alternated interactions.

Using a path integral formulation of the partition function based on spin coherent states, we analytically mapped the system into a NLσM plus a topological term. This allowed us to confirm [52,55,57] that, for a certain value of the parameter γ which characterizes the interaction, there is a phase transition. We note here that the numerical result for γ_c seems to be very close to half of our theoretical prediction. The same discrepancy was found for spin-1 chains with staggered interaction [49,76]. This effect may be due to different causes, such as lattice and finite-size effects, perturbative, and nonperturbative renormalization corrections to the semiclassical (large s) approximation on which the Haldane map is based, an implicit dependence on the number of legs. With our present knowledge, we are not able to sort these different effects out, but this does not affect our main findings.

We then performed a numerical study based on the DMRG algorithm to characterize the two different gapped phases. In particular, we saw that the $\gamma > \gamma_c$ phase is accompanied by a set of zero modes, hinting that it corresponds to an SPT order. This was confirmed by the analysis of the correlations between the spins at the edges and by looking at the degeneracy of the entanglement spectrum. We also calculated some NLOP, showing that the parity and the string order parameters have a dual behavior, with the former being nonzero for $\gamma < \gamma_c$ and the latter for $\gamma > \gamma_c$.

Following the classification of Refs. [27–29], we can say that we can identify the region for $\theta < \theta_c$ with a Mott insulatorlike phase and the region with $\theta > \theta_c$ with a Haldane insulatorlike phase.

In conclusion, our results show that the presence of a topological term in the NLσM induces a critical point which separates an ordinary phase from a topological one.

A similar situations may be encountered in other systems. For example, it would be interesting to extend this analysis to ladders with more than two legs, possibly going toward the two-dimensional limit. Also, an analogous study could be performed in the case of higher spin SU(2) [4,5] or even $SU(N)$ [77] systems.

ACKNOWLEDGMENTS

G.G., G.M., and E.E. are partially supported through the project ALMAIDEA by University of Bologna. G.M. and E.E. are partially supported through the project QUANTUM by Istituto Nazionale di Fisica Nucleare (INFN).

APPENDIX

In this Appendix, we give some details about the numerical analysis and, in particular, the finite-size scaling procedure we adopt. We perform the numerical analysis by means of a finite-size DMRG code which is based on TNs. The ITensor library [78] allows us to describe the wave function of a system by using a network of interconnected tensors. In this framework, matrix product states are TN states that correspond to a one-dimensional array of tensors [67–69]. In a similar way, operators as the Hamiltonian are represented by means of matrix product operators, yielding powerful tools to describe a wide range of models including one-dimensional chains and ladders. TN codes work better with OBCs than with PBCs. However, if it is necessary to analyze both boundary conditions, as we do, PBCs can be easily achieved from OBC code adding the appropriate interaction term between the first and last site of each chain in the Hamiltonian.

Since the ITensor Network Library does not implement the conservation of the total spin quantum number, our simulations are implemented in the whole Hilbert space and we target the ground state and the first three/four excited states. This multitarget approach allows us to check that the SU(2) symmetry is respected also at the level of numerical simulations, a fact which is also confirmed by the behavior of NLOP (Figs. 4 and 5) and spin correlation functions (Figs. 6–8).

We work with up to N sites for each chain, $N = 30$ for PBC and $N = 32$ for OBC; in the calculations of the energy spectrum we usually consider seven sweeps for each state, while for spin correlation functions we consider 40 sweeps. For each sweep, the maximum value of bond dimension varies from 10 to 500 and the minimum value of bond dimension varies from 10 to 20. Also, the cutoff changes from 10^{-5} to 10^{-10} and the noise term, which is added to the density matrix to help convergence, varies from 10^{-5} to 0.

All the physical quantities that we have evaluated (energy gap, NLOP, spin correlation functions, entanglement entropy, and spectrum) are consistent with the analytical prediction of a critical point γ_c and the emergence of two different phases. As already anticipated in Sec. III A, our aim is not the exact determination of the critical point γ_c, but the analysis of the two gapped phases, to show that the one for $\gamma > \gamma_c$ is topological. For completeness, however, here we present some graphs describing the finite-size behavior of the different physical quantities of interest.

First, we consider the scaling of the first four excited energy states close to the critical point. This is shown in Fig. 12 for both PBCs and OBCs, in the cases of $\gamma = 0.35$ and $\gamma = 0.4$. These data clearly indicate that we are very close to a phase transition point, whose accurate location would, however, require bigger sizes of the ladder to have results which are independent of boundary conditions.

Second, we describe how the NLOPs scale with the size of the system. In particular, since the SU(2) symmetry is respected, in the first two panels of Fig. 13 we only report the values of the z component of the parity and string order parameters as functions of γ, for different system sizes ($N = 16, 20, 24, 28, 32, 36$) and OBCs. Then, in the third panel, we show how the string order parameter scales to zero in the trivial phase, for $\gamma = 0.2$, while in the fourth panel we show how the parity order parameter scales to zero in the topological phase, for $\gamma = 0.8$.

All these data confirm that the maximum size at which we perform the numerical simulations ($N = 30$ for PBC and $N = 32$ for OBC) is large enough to ensure small errors and accuracy of the results.

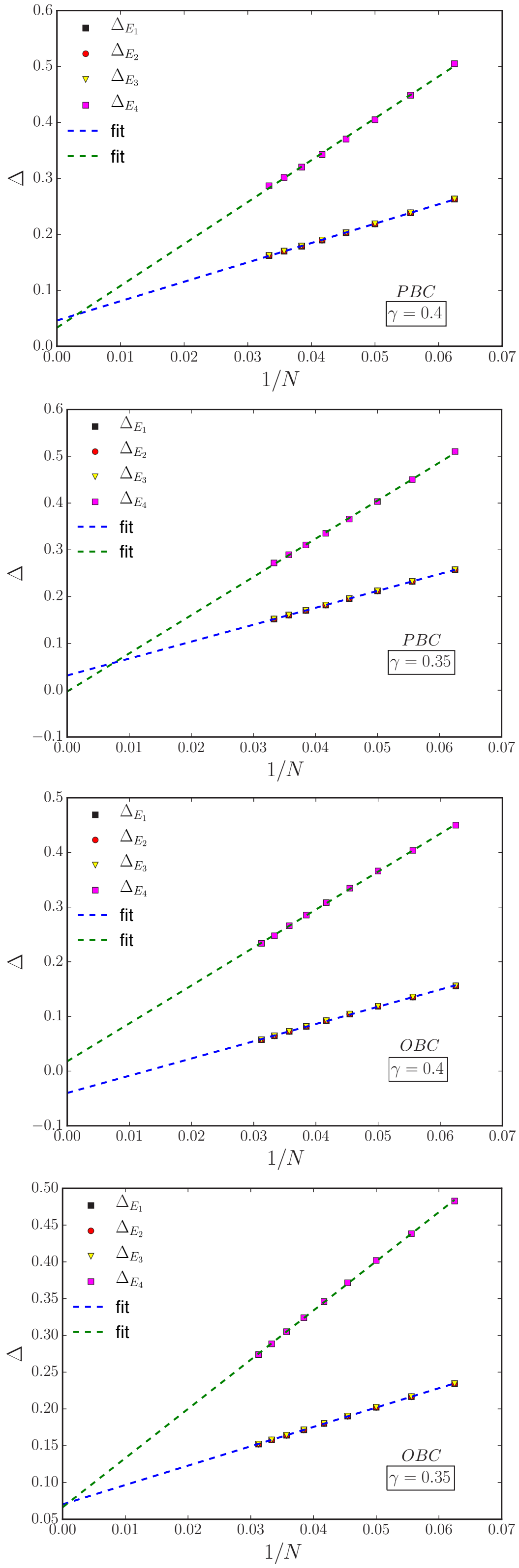

FIG. 12. Scaling of the energy gap of each state of the triplet Δ_{E_1}, Δ_{E_2}, Δ_{E_3} and of the energy gap of the fourth excited state Δ_{E_4} with respect to the ground state; we consider for PBCs $N = 16, 18, 20, 22, 24, 26, 28, 30$ sites on each chain and for OBCs $N = 16, 18, 20, 22, 24, 26, 28, 30, 32$ sites on each chain. First panel: PBC and $\gamma = 0.4$. Second panel: PBC and $\gamma = 0.35$. Third panel: OBC and $\gamma = 0.4$. Fourth panel: OBC and $\gamma = 0.35$.

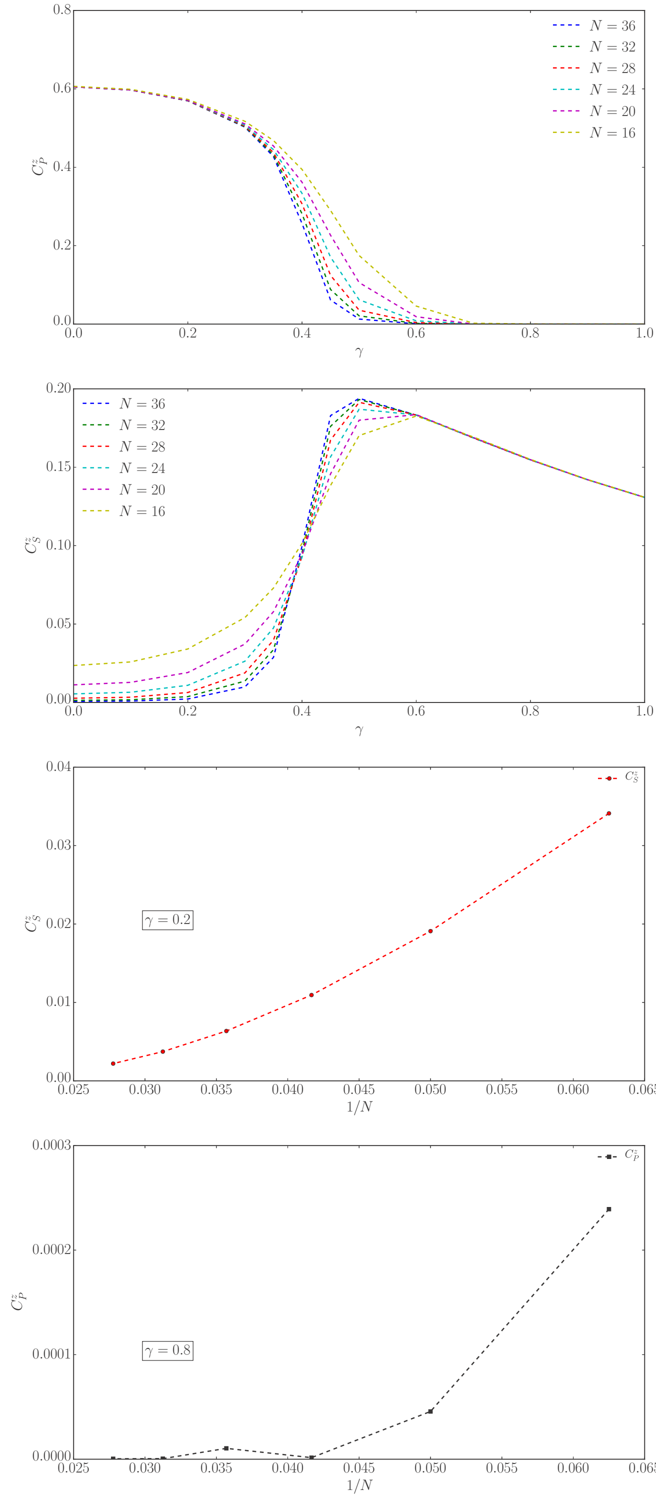

FIG. 13. Finite size-scaling of NLOP. First and second panel: parity C_P^z and string C_S^z order parameters, respectively, as function of γ, for OBC and different sizes. Third panel: string order parameter C_S^z, as function of $1/N$ in the trivial phase with $\gamma = 0.2$. Fourth panel: parity order parameter C_P^z, as function of $1/N$ in the topological phase with $\gamma = 0.8$.

[1] C. Degli Esposti Boschi, E. Ercolessi, G. Morandi, in *Low-Dimensional Spin Systems: Hidden Symmetries, Conformal Field Theories and Numerical Checks*, Symmetries in Science XI, edited by B. J. Gruber, G. Marmo, (Springer, Dordrecht, 2004).

[2] S. Sachdev, *Quantum Phase Transitions* (Cambridge University Press, Cambridge, 1998).

[3] R. J. Baxter, *Exactly Solved Models in Statistical Mechanics* (Academic Press, London, 1989).

[4] F. D. M. Haldane, Continuum dynamics of the 1-D Heisenberg antiferromagnet: Identification with the O(3) nonlinear sigma model, Phys. Lett. A **93**, 464 (1983).

[5] F. D. M. Haldane, Nonlinear Field Theory of Large-Spin Heisenberg Antiferromagnets: Semiclassically Quantized Solitons of the One-Dimensional Easy-Axis Néel State, Phys. Rev. Lett. **50**, 1153 (1983).

[6] J. R. Klauder and B. S. Skagerstam, *Coherent States* (World Scientific, Singapore, 1985).

[7] I. Affleck, in *Fields, Strings and Critical Phenomena*, edited by E. Brezin and J. Zinn-Justin (North-Holland, Amsterdam, 1990).

[8] R. Rajaraman, *Solitons and Instantons* (North-Holland, Amsterdam, 1982).

[9] G. Morandi, *The Role of Topology in Classical and Quantum Physics* (Springer-Verlag, Berlin, 1992).

[10] N. Read and S. Sachdev, Some features of the phase diagram of the square lattice SU(N) antiferromagnet, Nucl. Phys. B **316**, 609 (1989).

[11] A. M. Polyakov, Interaction of goldstone particles in two dimensions. Applications to ferromagnets and massive Yang-Mills fields, Phys. Lett. B **59**, 79 (1975).

[12] I. Affleck, T. Kennedy, E. H. Lieb, and H. Tasaki, Rigorous Results on Valence-Bond Ground States in Antiferromagnets, Phys. Rev. Lett. **59**, 799 (1987).

[13] I. Affleck, T. Kennedy, E. H. Lieb, and H. Tasaki, Valence bond ground states in isotropic quantum antiferromagnets, Commun. Math. Phys. **115**, 477 (1988).

[14] T. Kennedy and H. Tasaki, Hidden $Z_2 \times Z_2$ symmetry breaking in Haldane-gap antiferromagnets, Phys. Rev. B **45**, 304 (1992).

[15] V. L. Berezinskii, Destruction of long-range order in one-dimensional and two-dimensional systems possessing a continuous symmetry group. II. Quantum systems, Sov. Phys. JEPT **34**, 610 (1972).

[16] J. M. Kosterlitz and D. J. Thouless, Ordering, metastability and phase transitions in two-dimensional systems, J. Phys. C **6**, 1181 (1973).

[17] P. C. Hohenberg, Existence of long-range order in one and two dimensions, Phys. Rev. **158**, 383 (1967).

[18] N. D. Mermin and H. Wagner, Absence of Ferromagnetism or Antiferromagnetism in One- or Two-Dimensional Isotropic Heisenberg Models, Phys. Rev. Lett. **17**, 1133 (1966).

[19] L. Landau, On the theory of phase transitions, Zh. Eksp. Teor. Fiz. **7**, 19 (1937).

[20] Z.-C. Gu and X.-G. Wen, Tensor-entanglement-filtering renormalization approach and symmetry-protected topological order, Phys. Rev. B **80**, 155131 (2009).

[21] A. P. Schnyder, S. Ryu, A. Furusaki and A. W. W. Ludwig, Classification of topological insulators and superconductors in three spatial dimensions, Phys. Rev. B **78**, 195125 (2008).

[22] A. Kitaev, Periodic table for topological insulators and superconductors, AIP Conf. Proc. **1134**, 22 (2009).

[23] X.-G. Wen, Symmetry-protected topological phases in noninteracting fermion systems, Phys. Rev. B **85**, 085103 (2012).

[24] L. Fidkowski and A. Kitaev, Effects of interactions on the topological classification of free fermion systems, Phys. Rev. B **81**, 134509 (2010).

[25] M. Z. Hasan and C. L. Kane, Colloquium: Topological insulators, Rev. Mod. Phys. **82**, 3045 (2010).

[26] X.-L. Qi and S.-C. Zhang, Topological insulators and superconductors, Rev. Mod. Phys. **83**, 1057 (2011).

[27] A. Montorsi and M. Roncaglia, Nonlocal Order Parameters for the 1D Hubbard Model, Phys. Rev. Lett. **109**, 236404 (2012).

[28] L. Barbiero, A. Montorsi, and M. Roncaglia, How hidden orders generate gaps in one-dimensional fermionic systems, Phys. Rev. B **88**, 035109 (2013).

[29] A. Montorsi, F. Dolcini, R. C. Iotti, and F. Rossi, Symmetry-protected topological phases of one-dimensional interacting fermions with spin-charge separation, Phys. Rev. B **95**, 245108 (2017).

[30] T. Giamarchi, *Quantum Physics in One Dimension*, Vol. 121 of International Series of Monographs on Physics, (Oxford University Press, Clarendon, 2004).

[31] F. D. M. Haldane, O(3) Nonlinear σ Model and the Topological Distinction Between Integer- and Half-Integer-Spin Antiferromagnets in Two Dimensions, Phys. Rev. Lett. **61**, 1029 (1988).

[32] E. Fradkin and M. Stone, Topological terms in one- and two-dimensional quantum Heisenberg antiferromagnets, Phys. Rev. B **38**, 7215 (1988).

[33] L. B. Ioffe and A. I. Larkin, Effective action of a two-dimensional antiferromagnet, Int. J. Mod. Phys. B **2**, 203 (1988).

[34] T. Dombre and N. Read, Absence of the Hopf invariant in the long-wavelength action of two-dimensional quantum antiferomagnets, Phys. Rev. B **38**, 7181 (1988).

[35] A. Angelucci and G. Jug, Novel path integral approach to effective field theories for D-dimensional quantum spin systems, Int. J. Mod. Phys. B **3**, 1069 (1989).

[36] T. M. Rice, S. Golapan, and M. Sigrist, Superconductivity, spin gaps and Luttinger liquids in a class of cuprates, Europhys. Lett. **23**, 445 (1993).

[37] E. Dagotto, J. Riera, and D. Scalapino, Superconductivity in ladders and coupled planes, Phys. Rev. B **45**, 5744 (1992).

[38] E. Dagotto, Correlated electrons in high-temperature superconductors, Rev. Mod. Phys. **66**, 763 (1994).

[39] D. C. Johnston, J. W. Johnson, D. P. Goshorn, and A. J. Jacobson, Magnetic susceptibility of $(VO)_2P_2O_7$: A one-dimensional spin-1/2 Heisenberg antiferromagnet with a ladder spin configuration and a singlet ground state, Phys. Rev. B **35**, 219 (1987).

[40] Z. Hiroi, M. Azuma, M. Takano, and Y. Bando, A new homologous series $Sr_{n-1}Cu_{n+1}O_{2n}$ found in the SrOCuO system treated under high pressure, J. Solid State Chem. **95**, 230 (1991).

[41] M. Azuma, Z. Hiroi, M. Takano, K. Ishida, and Y. Kitaoka, Observation of a Spin Gap in $SrCu_2O_3$ Comprising Spin-$\frac{1}{2}$ Quasi-1D Two-Leg Ladders, Phys. Rev. Lett. **73**, 3463 (1994).

[42] T. Barnes and J. Riera, Susceptibility and excitation spectrum of $(VO)_2P_2O_7$ in ladder and dimer-chain models, Phys. Rev. B **50**, 6817 (1994).

[43] E. Dagotto and T. M. Rice, Surprises on the way from one- to two- dimensional quantum magnets: The ladder materials, Science **271**, 618 (1996).

[44] D. V. Khveshchenko, Singlet pairing in the doublet-chain *t-J* model, Phys. Rev. B **50**, 380 (1994).

[45] D. Sénéchal, Semiclassical description of spin ladders, Phys. Rev. B **52**, 15319 (1995).

[46] D. G. Shelton, A. A. Nersesyan and A. M. Tsvelik, Antiferromagnetic spin ladders: Crossover between spin $S = 1/2$ and $S = 1$ chains, Phys. Rev. B **53**, 8521 (1996).

[47] S. Dell'Aringa, E. Ercolessi, G. Morandi, P. Pieri, and M. Roncaglia, Effective Actions for Spin Ladders, Phys. Rev. Lett. **78**, 2457 (1997).

[48] G. Sierra, The nonlinear sigma model and spin ladders, J. Phys. A: Math. Gen. **29**, 3299 (1996).

[49] G. Sierra, *Lectures Notes in Physics*, Vol. 478, edited by G. Sierra and M. A. Martin-Delgado (Springer-Verlag, Berlin, 1997).

[50] L. Campos Venuti, C. Degli Esposti Boschi, E. Ercolessi, F. Ortolani, G. Morandi, S. Pasini, and M. Roncaglia, Particle content of the nonlinear sigma model with theta-term: A lattice model investigation, J. Stat. Mech. (2005) L04004.

[51] M. Sato, N-leg integer-spin ladders and tubes in commensurate external fields: Nonlinear sigma model approach, Phys. Rev. B **72**, 104438 (2005).

[52] M. A. Martin-Delgado, R. Shankar, and G. Sierra, Phase Transitions in Staggered Spin Ladders, Phys. Rev. Lett. **77**, 3443 (1996).

[53] G. Magnifico, D. Vodola, E. Ercolessi, S. P. Kumar, M. Müller, and A. Bermudez, Symmetry-protected topological phases in lattice gauge theories: Topological QED_2, Phys. Rev. D **99**, 014503 (2019).

[54] G. Magnifico, D. Vodola, E. Ercolessi, S. P. Kumar, M. Müller, and A. Bermudez, Z_N gauge theories coupled to topological fermions: QED_2 with a quantum-mechanical θ angle, Phys. Rev. B **100**, 115152 (2019).

[55] M. A. Martin-Delgado, J. Dukelsky, and G. Sierra, Phase diagram of the 2-leg Heisenberg ladder with alternating dimerization, Phys. Lett. A **250**, 430 (1998).

[56] N. J. Robinson, A. Altland, R. Egger, N. M. Gergs, W. Li, D. Schuricht, A. M. Tsvelik, A. Weichselbaum, and R. M. Konik, Nontopological Majorana Zero Modes in Inhomogeneous Spin Ladders, Phys. Rev. Lett. **122**, 027201 (2019).

[57] N. Chepiga, F. Michaud, and F. Mila, Berry phase investigation of spin-*S* ladders, Phys. Rev. B **88**, 184418 (2013).

[58] K. Totsuka and M. Suzuki, The spin-1/2 Heisenberg spin ladder with bond alternation, J. Phys.: Condens. Matter **7**, 6079 (1995).

[59] A. Auerbach, *Interacting Electrons and Quantum Magnetism*, 2nd ed. (Springer-Verlag, New York, 1998).

[60] E. Fradkin, *Field Theories of Condensed Matter Systems,* 1st ed. (Addison-Wesley, Redwood City, 1991).

[61] M. Greven, R. J. Birgeneau, and U.-J. Wiese, Monte Carlo Study of Correlations in Quantum Spin Ladders, Phys. Rev. Lett. **77**, 1865 (1996).

[62] S. R. White, R. M. Noack, and D. J. Scalapino, Resonating Valence Bond Theory of Coupled Heisenberg Chains, Phys. Rev. Lett. **73**, 886 (1994).

[63] G. Ghelli, Topological phases in spin ladders, Master Thesis, University of Bologna, 2018, https://amslaurea.unibo.it/17050/

[64] R. Shankar and N. Read, The $\theta = \pi$ nonlinear sigma model is massless, Nucl. Phys. B **336**, 457 (1990).

[65] S. R. White, Density-matrix algorithms for quantum renormalization groups, Phys. Rev. B **48**, 10345 (1993).

[66] S. R. White, Density Matrix Formulation for Quantum Renormalization Groups, Phys. Rev. Lett. **69**, 2863 (1992).

[67] F. Verstraete, V. Murg, and J. I. Cirac, Matrix product states, projected entangled pair states, and variational renormalization group methods for quantum spin systems, Adv. Phys. **57**, 143 (2008).

[68] U. Schollwöck, The density-matrix renormalization group in the age of matrix product states, Ann. Phys. **326**, 96 (2011).

[69] R. Orús, A practical introduction to tensor networks: Matrix product states and projected entangled pair states, Ann. Phys. **349**, 117 (2014).

[70] E. O. Gogolin, E. A. Nersesyan, and M. Tsvelik, *Bosonization and Strongly Correlated Systems* (Cambridge University Press, Cambridge, 1998).

[71] S. Fazzini, F. Becca, and A. Montorsi, Nonlocal Parity Order in the Two-Dimensional Mott Insulator, Phys. Rev. Lett. **118**, 157602 (2017).

[72] C. Degli Esposti Boschi, A. Montorsi, and M. Roncaglia, Brane parity orders in the insulating state of Hubbard ladders, Phys. Rev. B **94**, 085119 (2016).

[73] L. Campos Venuti, C. Degli Esposti Boschi, and M. Roncaglia, Long-Distance Entanglement in Spin Systems, Phys. Rev. Lett. **96**, 247206 (2006).

[74] T. J. Osborne and F. Verstraete, General Monogamy Inequality for Bipartite Qubit Entanglement, Phys. Rev. Lett. **96**, 220503 (2006).

[75] F. Pollmann, A. M. Turner, E. Berg, and M. Oshikawa, Entanglement spectrum of a topological phase in one dimension, Phys. Rev. B **81**, 064439 (2010).

[76] S. Yamamoto, Ground-state properties of $S = 1$ antiferromagnetic Heisenberg chains with bond alternation, J. Phys. Soc. Jpn. **63**, 4327 (1994).

[77] I. Affleck, Large-*n* Limit of SU(n) Quantum "Spin" Chains, Phys. Rev. Lett. **54**, 966 (1985).

[78] ITensor Library, version 2.1.1, http://itensor.org